Original Research Article

Human and Experimental Toxicology
Volume 41: 1–12

DOI: 10.1177/09603271221143029
journals.sagepub.com/home/het

The protective effects of red ginseng and amifostine against renal damage caused by ionizing radiation

Hamit Yilmaz[1], Yunus Karakoc[2], Levent Tumkaya[3], Tolga Mercantepe[3], Hacer Sevinc[3], Adnan Yilmaz[4] and Sema Yılmaz Rakıcı[5]

Abstract

This study aimed to elucidate the effects of amifostine (ethyol) (AM), a synthetic radioprotector, and red ginseng (RG), a natural radioprotective agent, against the toxic effect of ionizing radiation (IR) on kidney tissues through changes in biochemical and histopathological parameters in addition to contributions to the use of amifostine and RG in clinical studies. Five groups were established: Group I (control, receiving only saline by gavage), Group II (IR only), and Group III (IR+AM, 200 mg/kg intraperitoneally (i.p.). Group IV (IR + RG, 200 mg/kg orally once a day for 4 weeks), and Group V (IR+RG+AM, 200 mg/kg orally once/day for 4 weeks before IR and 200 mg/kg AM administered (i.p.) 30 min before IR). All groups, except for the control group, were subject to 6-Gy whole-body IR in a single fraction. 24 h after irradiation, all animals were sacrificed under anesthesia. IR enhanced MDA, 8-OHdG, and caspase-3 expression while decreasing renal tissue GSH levels ($p < .05$). Significant numbers of necrotic tubules together with diffuse vacuolization in proximal and distal tubule epithelial cells were also observed. The examination also revealed substantial brush boundary loss in proximal tubules as well as relatively unusual glomerular structures. While GSH levels significantly increased in the AM, RG, and AM+RG groups, a decrease in KHDS, MDA, 8-OHdG, and caspase-3 expression was observed, compared to the group subject to IR only ($p < .05$). Therefore, reactive oxygen species-scavenging antioxidants may represent a promising treatment for avoiding kidney damage in patients receiving radiation.

Keywords

Amifostine, ionizing radiation, kidney, oxidative stress, red ginseng

Introduction

Cancer is among the most serious threats to public health, with a high incidence and mortality rate worldwide.[1] Therapeutic approaches have been extensively investigated.[2,3] Radiation therapy (RT), the most often used approach, is employed alone in the treatment of malignant tumor cells and in combination with other treatments.[4–6] RT is applied in approximately 60% of cancer cases. Despite its importance in treatment, it can cause local and systemic problems.[3,7]

Renal tissues are most affected by local or total body irradiation used in the treatment of gastrointestinal tumors, gynecological cancers, lymphomas, and upper

[1]Department of Biophysics, Faculty of Medicine, University of Health Sciences, Istanbul, Turkey
[2]Department of Biophysics, Faculty of Medicine, University of Health Sciences, Istanbul, Turkey
[3]Department of Histology and Embryology, Faculty of Medicine, Recep Tayyip Erdogan University Rize, Turkey
[4]Department of Medical Biochemistry, Faculty of Medicine, Recep Tayyip Erdogan University Rize, Turkey
[5]Department of Radiation Oncology, Faculty of Medicine, Recep Tayyip Erdogan University Rize, Turkey

Corresponding author:
Hamit Yilmaz, Department of Biophysics, Faculty of Medicine, University of Health Sciences, Istanbul, Turkey, 53100, Turkey.
Email: hamit.yilmaz@erdogan.edu.tr

abdominal sarcomas. Kidney tissue must therefore be considered in dosage calculation, which exhibits high radiosensitivity.[8] Previous research has established that oxidative stress occurring in tissues after radiation triggers apoptosis in renal tubular cells.[9,10] Although the severity of radiation damage varies with age and dose, the kidney can tolerate roughly equivalent to a high dose rate single dose of 4-5 Gy.[11,12] Studies have also reported vascular permeability, deterioration in perfusion, inflammation reaction, and fibrosis in the kidney as a result of radiation.[13] Histopathological studies of IR-induced nephropathy have reported damage to the kidney glomeruli, blood vessels, tubular epithelium, and interstitium.[14] Reversible renal cell injury can result in systemic inflammation and long-lasting nephropathy.[15] Oxidative stress in kidney damage caused by IR also causes a drop in the components needed for body homeostasis. This in turn leads to impaired kidney function.[16] It is therefore essential to protect the kidneys against IR damage.

Ionizing radiation (IR) leads to oxidative stress by increasing levels of cell-damaging free radicals and harmful chemicals.[12] Reactive oxygen species (ROS) cause infection and activation of transcription factors, resulting in DNA damage and chain breakage.[17] If this damage to the cell is not repaired, apoptosis is initiated.[9] Radiation-induced ROS increases malondialdehyde (MDA) levels while drastically lowering those of glutathione (GSH) and reducing antioxidant capability.[18,19]

Therefore, new protective procedures and radioprotective substances must be developed to limit and/or eliminate the adverse consequences described above. Antioxidants have been the focus of considerable research for protecting cells from tissue damage caused by oxidative stress.[9] The most commonly used synthetic radio protectant, amifostine (AM), mitigates the effect of radiation on tumor tissue while sparing healthy tissues. AM used before radiotherapy or chemotherapy accumulates more rapidly in normal tissues compared to tumor tissues. AM is thus able to protect normal tissue more than 100 times better than it does malignant tissue.[20] Despite its inherent toxicity, AM is still indispensable due to its success in tumor treatment.[21] Red ginseng (RG) is a widely used natural radioprotectant, which has been used in Far Eastern medicine for more than 2000 years due to its antioxidant and anti-inflammatory properties. The radioprotective effects of ginseng might be closely associated with its antioxidative and immunomodulating capabilities. It is also a powerful adaptogen that creates resistance to stress and aging.[22,23]

The purpose of this study was to investigate the impact of the synthetic radioprotector AM and of the natural radioprotective agent RG against the harmful effects of IR on healthy kidney tissues by examining changes in biochemical and histopathological markers. Another aim was to contribute to the use of AM and RG in the clinical setting.

Materials and methods

Animals and experimental design

Forty male Sprague Dawley rats, 12–14 weeks old and weighing 200 ± 15 g, were obtained from the Recep Tayyip Erdoğan University (RTEU) Animal Care and Research Unit (Rize, Turkey) were used in the study. All animals were cared for by the principles outlined in the National Institutes of Health Guidelines for the Care and Use of Laboratory Animals (IACUC). The RTEU Local Animal Care Committee approved the study (2020/38–30.10.2020).

Rats were allocated into five groups, one control and four experimental. The control received saline solution only by oral gavage for 29 days. Previous studies showed that a dose of 6 Gy total-body irradiation resulted in nephrotoxicity. Therefore, we adopted this application.[10,12,24] The IR group was exposed to a single dose of 6 Gy whole-body radiation on the 29th day following saline administration by oral gavage for 28 days.[10,12,25] The rats were sacrificed on day 30. The rats in the IR+AM group first received saline solution by gavage for 28 days. On the 29th day, they received one dose of 200 mg/kg AM via the i.p. 30 min before administration of 6 Gy x-irradiation.[21,26,27] The IR+RG group received 200 mg/kg RG by gavage for 29 days.[22,23,28] On the 29th day, they were administered one dose of total-body x-irradiation and were sacrificed on day 30. The IR+RG+AM rats received 200 mg/kg RG by gavage for 29 days. On the 29th day, they received one dose of 200 mg/kg AM i.p. 30 min before administration of 6 Gy x-irradiation. The rats were then sacrificed under anesthesia on day 30.

All rats were kept in cages holding eight rats under optimum laboratory conditions (50–55% humidity, 22 ± 2°C temperature, and a 12:12 h light: dark cycle, ad libitum same water and food pellets). Weight was monitored weekly throughout the study.

Chemicals

Radiation (IR) and sacrifice procedures were performed after the rats had been anesthetized. Anesthesia was induced with intramuscular ketamine (100 mg/kg, Pfizer Pharma, Istanbul, Turkey) and xylazine (3.9 mg/kg, Interhas A.Ş., Istanbul, Turkey). Amifostine (200 mg/kg) was obtained from ER-KIM Pharma (Istanbul, Turkey) and RG in 99% pure powder form was provided by Aksu Vital Natural Products Food Industry and Trade Inc. (Istanbul, Turkey). Sigma Chemical Co. and Merck supplied all chemical compounds for laboratory experiments (Germany).

Irradiation procedure

Following the induction of anesthesia, rats were immobilized in the prone position. The rats were irradiated by the isometric method with 6 MV from the back and front using a bolus of 1 cm in an area of 20 cm × 40 cm, and a gantry of 0 and 180 degrees. A digital linear accelerator (Elekta Synergy; Elekta, Crawley, United Kingdom) was used at 6 MV at a dose rate of 4 Gy/min. to apply Photon irradiation (X-ray) The CMS-XIO radiotherapy treatment planning system (version 13.2) was employed. In this study, the animals were treated daily with 6-Gy single-fraction RT in the whole body and sacrificed 24 h after irradiation[10,12,25]

Biochemical procedure

Tissue extraction and homogenization. Kidney tissue samples were homogenized on ice for a few minutes at 9500 r/min by adding 9 mL of working solution (0.15 M KCl) to 1 g sample. The homogenates were then transferred to Eppendorf tubes and pelleted at 4000xg for 10 min at +4°C for supernatant separation.[8,29] MDA and GSH levels in the supernatants were measured spectrophotometrically.

Determination of malondialdehyde (MDA) concentrations. MDA was measured spectrophotometrically. Following incubation, 900 µL was removed from the working tubes, mixed with 600 µL of TCA solution, and centrifuged at 3000 r/min for 10 min. Then, 900 µL of supernatant was added to 300 µL of freshly made TBA solution, and the resulting mixture was incubated in boiling water for 15 min. Absorbance was calculated at 532 nm, and lipid peroxide contents were expressed as nmol/g tissue.[30,31]

Determination of total thiol. For the determination of GSH in kidney tissue, the -SH groups were determined using the Ellman's method of total thiol determination.[32] The following processes were used in the analysis, in the sequence given: Ellman's reagent was prepared by dissolving 4 mg of Dithiobis 2 nitrobenzoic acid (DTNB) in 10 mL of 1% sodium citrate solution. Next steps, 100 µL of 3 M Na_2HPO_4, and 25 µL of DTNB solution and vortexed onto 25 µL of kidney supernatant. A wavelength of 412 nm was used to read the yellow color on the spectrophotometer. The results were determined with a prepared 1000 µM–62.5 µM reduced glutathione standard graph and calculated as mmol/gr tissue.[14]

Histopathological analysis. After the end of the experiment, animals were eviscerated and specimens from the renal tissues were collected. The kidney tissues were trimmed (1.5 cm^3) and fixed in a 10% neutral buffered formalin (Sigma-Aldrich, Saint Louis, MO, USA) solution for 36 h. Tissue samples obtained using a tracking device (Shandon Citadel 2000, Thermo Scientific, Germany) by routine histological tissue procedures were then dehydrated in ascending grades ethanol (Merck GmbH, Darmstadt, Germany) series, followed by two series of xylol solutions (Merck GmbH, Darmstadt, Germany).[10,18,33] The samples were then embedded (Isolab GmbH, Germany) in tissue embedding (Leica, EG1150, Germany) cassettes using an embedding device. Next, 4-5 µm sections were taken using a rotary microtome (Leica RM2525, Germany), stained with Harris Hematoxylin and Eosin G (Merck GmbH, Darmstadt, Germany) using an autotechnic device. They were analyzed under a light microscope (Olympus BX51, Olympus Corp., Japan) using a digital camera (Olympus DP71, Olympus Corp., Japan) attachment and photographed.[12]

Immunohistochemical (IHC) analysis. Kidney tissue specimens were incubated using a TUNEL kit (ab206386, Abcam, UK), and Anti-Caspase-3 primary antibody (ab184787, Abcam, UK) and 8-OHdG primary antibody (SC66036, Santa Cruz Biotechnology Inc., Dallas, TX, USA) kits. In addition, sections of kidney tissue incubated with secondary antibodies which are suitable for primary antibodies were applied with the help of the Leica Bond Max IHC/ISH stainer (Leica microsystem, Melbourne, Australia). Sections were stained through Harris Hematoxylin for counterstaining (Merck GmbH, Darmstadt, Germany).[14,30]

Semi-quantitative analysis. Histopathological findings in sections of H&E stained kidney tissue were evaluated as described,[33] while tubular necrosis histopathological injury scoring was performed, as stated previously via Brush border losses in proximal tubule epithelial cells, vacuolation in tubular epithelial cells and atypical glomeruli findings.[10] Renal histopathological damage scoring was modified and scored as shown in Supplementary Table 1. Positive cells in sections were scored on a four-point scale from 0 to 3 for cell numbers exhibiting signs of IHC positivity (0: 5%, 1: ≥6–25%, 2: ≥26–50%, 3: ≥50). Two histopathologists (TM and LT) blinded to the research group data graded semi-quantitative analyses, using 20 different randomly chosen areas on sections taken from each rat at ×20 magnification.

Statistical analysis. The biochemical, semi-quantitative, and histopathological data yielded by this study were analyzed on SPSS 20.00 (IBM Corp. Chicago, IL, USA) statistical software. Levene's test, skewness-kurtosis, Q-Q plot, and Shapiro-Wilk test were performed to evaluate the conformity of the data with normal distribution. Parametric data were shown as arithmetic mean ± standard deviation values, and divergences between the groups were analyzed by Tukey's HSD and One-Way ANOVA tests. Nonparametric

Table 1. Biochemistry analysis results (arithmetic mean ± standard deviation).

Group	MDA (nmol/mg tissue)	GSH (total Thiol) (nmol/mg tissue)
Control	65.17 ± 2.90	11.42 ± 1.34
IR	79.89 ± 2.88[a]	7.05 ± 1.26[a]
IR+AM	74.12 ± 3.37[b,e]	8.97 ± 1.22[f,h]
IR+RG	72.83 ± 4.33[c,f]	9.4 ± .28[g,i]
IR+AM+RG	71.84 ± 5.72[d,e]	8.82 ± 0.84[b,j]

[a]p = .000; Compared to the control group.
[b]p = .001; Compared to the control group.
[c]p = .004; Compared to the control group.
[d]p = .016; Compared to the control group.
ep = .048; Compared to the IR group.
fp = .009; Compared to the IR group.
ep = .002; Compared to the IR group.
[f]p = .002; Compared to the control group.
[g]p = .015; Compared to the control group.
[h]p = .024; Compared to the control group.
[i]p = 0.004; Compared to the IR group.
[j]p = 0.043; Compared to the IR group.
One-Way ANOVA/Tukey HSD.

data were expressed as median values and an interquartile range of 25%–75%, and differences between the groups were assessed by the Tamhane T2 and Kruskal Wallis tests. Statistically, a significant p-value was accepted as <0,05.

Results

Biochemical results

MDA levels in kidney tissue, evaluated to assess lipid peroxidation, were found considerably higher in the IR group than those in the control group (Table 1; p = .000). On the contrary, renal tissue MDA levels were found considerably lower in the treatment groups that received AM and RG alone, or AM+RG in combination, compared to the IR group (Table 1; p = .048, p = .009, and p = .048, respectively).

Total thiol levels in kidney tissue, measured to determine tissue antioxidant levels, were decreased significantly in the IR group, compared to the control group (Table 1; p = .000). On the contrary, total thiol levels increased significantly in the AM-only, RG-only, and AM+RG combined treatment groups, compared to the IR group (Table 1; p = .024, p = .004, and p = .043, respectively).

Histopathological results

On light microscopic examination of H&E stained kidney tissue sections taken from the control group, it was determined that the epithelial cells of the glomeruli and proximal and distal tubules were normal in architecture (Table 2; Figures 1(a) and (b); RHDS: 0(0–1)). The brush border structures of the proximal tubules were also clearly visible. In contrast, diffuse vacuolization and diffuse coagulative necrotic tubules were observed in epithelial cells of the proximal and distal tubules in the IR group. Consistent brush boundary losses were also determined in the proximal tubules, together with moderately atypical glomerular structures (Table 2; Figure 1(c) and (d); RHDS: 7(5–7)). In contrast, a decrease in vacuolizations in tubular epithelial cells, atypical glomeruli, and loss of brush border structures of the proximal tubules were observed in the AM treatment group (Table 2; Figure 1(e) and (f); RHDS: 2(2–3)). Similarly, a decrease in the vacuolization of proximal and distal tubule epithelial cells, as well as a decrease in necrotic tubules were observed in the RG group. A decrease was also observed in brush border losses and atypical glomerular structures in the epithelial cells of the proximal tubular cells (Table 2; Figure 1(g) and (h); RHDS: 3(2–3)). Despite a decrease in necrotic tubules and abnormal glomerular structures in the IR+AM+RG combined treatment group, typical proximal and distal tubule structures were frequently observed (Table 2; Figure 1(i) and (j); RHDS: 1.5(1-2). In addition, we found that the loss of brush border structure in proximal tubule cells in the IR+AM+RG group was significantly reduced compared to the IR+RG group (Table 2; Figure 1(a) and (b); p = 0.014). Again, we observed that the vacuolizations in tubular epithelial cells in the IR+AM+RG group decreased compared to the

Table 2. Renal histopathological damage scoring (RHDS) analysis results (median (25%–75% interquartile range).

Groups	Loss of brush border of epithelial cells in proximal tubules	Vacuolization of tubular epithelial cells	Atypical glomeruli	RHDS
Control	0(0–0.5)	0(0-0)	0(0-0)	0(0-1)
IR	3(2-3)[a]	3(2-3)[a]	1(1-2)[a]	7(5–7)[a]
IR+AM	1(1-1)[a,b]	3(2-3)[a,b]	0(0-1)[e]	2(2-3)[a,b]
IR+RG	1(0-1)[a,b]	1(1-1)[a,b]	0(0-1)[e]	3(2-3)[a,b]
IR+AM+RG	0.5(0-1)[b,c]	0(0-1)[b,d]	0(0-1)[b,d,f]	1.5(1-2)[a,b,g,h]

[a]p = .000; Compared to the control group.
[b]p = .000; Compared to the IR administration group.
cp = .014; Compared to the IR+RG treatment grup.
dp = .007; Compared to the IR+AM treatment grup.
ep = .024; Compared to the IR administration roup.
[f]p = .04; Compared to the IR administration group.
[g]p = .002; Compared to the IR+AM treatment group.
[h]p = .000; Compared to the IR+RG treatment group.
Kruskal Wallis/Tamhane T2 test.

IR+AM group (Table 2; Figure 1(a) and (b); p = 0.007). We found that IR+AM group (RHDS: 2(2–3) and IR+RG group (RHDS: 3(2–3)) RHDS scores decreased in the IR+AM+RG group (RHDS: 1.5(1–2)) (Table 2; Figure 1(a) and (b); respectively: p = 0.002; p = 0.00).

Immunohistochemical results

Apoptotic cells exhibiting TUNEL positivity in proximal and distal tubule epithelial cells increased significantly, compared to the control group following IR (Table 3; Figure 2(a) and (b); p = 0.000). On the contrary, TUNEL positivity in tubular epithelial cells was lower in the AM treatment group than that in the IR group (Table 3; Figure 2(b) and (c); p = .000). Similarly, analysis of sections from the RG treatment group revealed significantly lower TUNEL positivity in the proximal and distal tubules than that in the IR group (Table 3; Figure 2(b) and (d); p = .000). As a result of light microscopic examination of kidney tissue sections from the IR+AM+RG group, a decrease was found in cells showing TUNEL positivity in the proximal and distal tubule epithelial cells, compared to the IR group (Table 3; Figure 2(b) and (e); p = .000).

Light microscopic examination of kidney tissues incubated with caspase-3 revealed a much larger number of cells showing caspase-3 positivity due to IR in the proximal and distal tubule epithelial cells, compared to the control group (Table 3; Figure 3(a) and (b); p = .000). In contrast, caspase-3 positivity in tubular epithelial cells decreased in the AM group compared to the IR group (Table 3; Figure 3(b) and (c); p = .000). Similarly, examination of kidney tissue sections from the RG group revealed much lower caspase-3 positivity in the proximal and distal tubules than in the IR group (Table 3; Figure 3(b) and (d); p = .000). Light microscopic examination of kidney tissue sections from the IR+AM+RG group revealed a decrease in cells exhibiting caspase-3 positivity in the proximal and distal tubule epithelial cells compared to the IR group (Table 3; Figure 3(b) and (e); p = .000).

Examination of sections incubated with 8-OHdG primary antibody under light microscopy revealed a significant increase in cells showing 8-OHdG positivity due to IR in the proximal and distal tubule epithelial cells, compared to the control group (Table 3; Figure 4(a) and (b); p = .01). In contrast, 8-OHdG positivity in tubular epithelial cells was higher in the IR group than in the AM group (Table 3; Figure 4(b) and (c); p = .000). Similarly, analysis of sections from the RG group revealed much lower 8-OHdG positivity in the proximal and distal tubules than in the IR group (Table 3; Figure 3(b) and (d); p = .000). Light microscopic examination of kidney tissue sections taken from the IR+AM+RG group showed a decrease in cells exhibiting 8-OHdG positivity in the proximal and distal tubule epithelial cells, compared to the IR group (Table 3; Figure 4(b) and (e); p = .000).

Discussion

Although contemporary RT procedures improve cancer treatment cure rates and local control, they have not eliminated the deleterious effects of IR on normal tissues. There are limited studies on the effect of IR on the kidney, a dose-limiting, and radiosensitive organ. The present study examines the acute effects of x-ray irradiation on kidney tissue by examining the damage mechanisms using histopathological, biochemical, and immunocytochemical (8-OHdG, Caspase-3, and Tunel) analysis methods. This is the first study to address the possible protective effects of AM and RG. Talebpour Amiri et al. (2018) reported that 2-Gy whole-body single fraction IR exposure resulted in

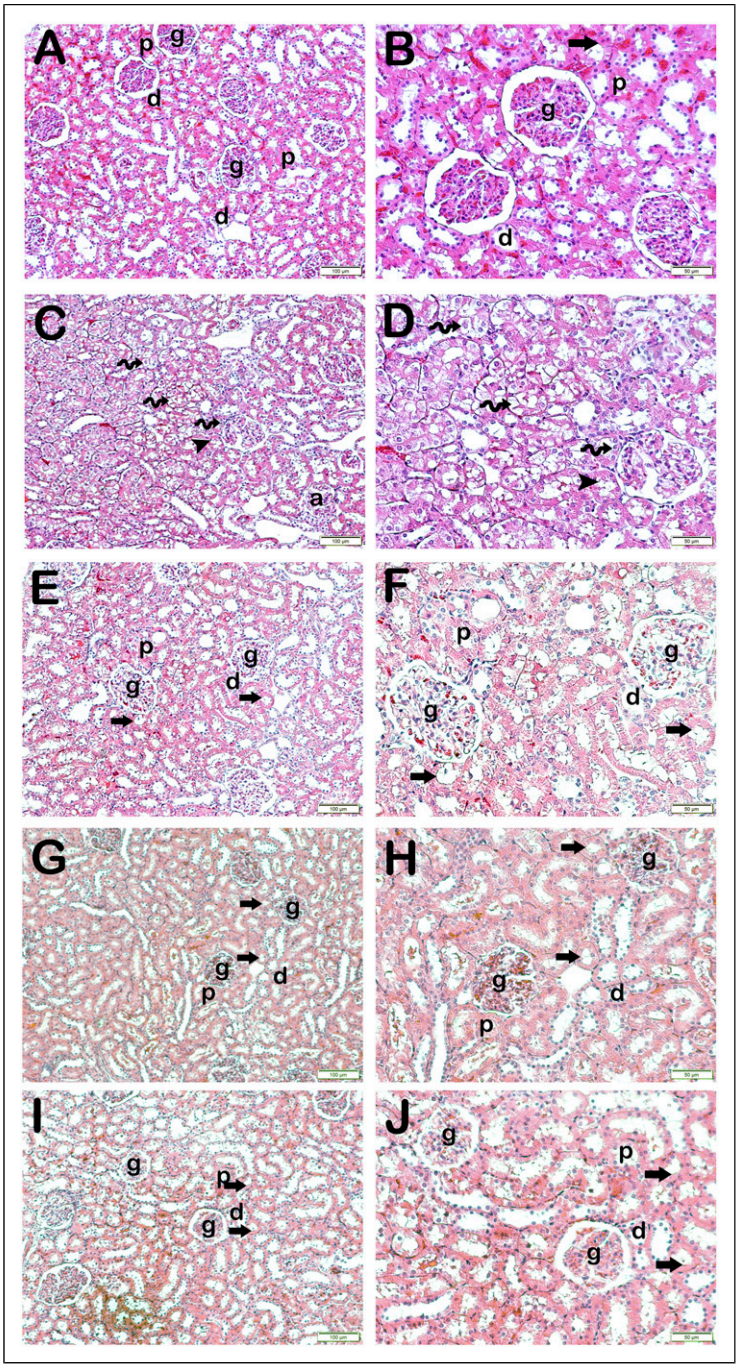

Figure 1. Representative light microscopic images of sections belonging to kidney tissue. Glomerule (g), Proximal tubule (p), Distal tubule (d), Brush border (arrow). (a) (x20)–(b) (x40): In the sections of the control group, it is observed that the glomeruli, proximal and distal tubules are in a normal structure. In addition, it is observed that brush border structures are prominent in proximal tubule epithelial cells (RHDS: 0(0–1)). (c) (x20)–(d) (x40): In sections belonging to the IR group, necrotic tubules accompanying diffuse vacuolizations (spiral arrow) are observed in tubule epithelial cells. Furthermore, the brush boundary (arrowhead) and atypical glomeruli (a) are lost in the proximal tubule epithelial cells (RHDS: 7(5–7)). (e) (x20)–(f) (x40): A reduction in necrotic tubules and atypical glomerular structures was observed in the AM treatment group. Additionally, there are fewer losses in the brush border structures of the proximal tubules, and typical brushy boundary structures (arrow) are detected (RHDS: 2(2–3)). (g) (x20)–(h) (x40): It is observed that atypical glomeruli, vacuolization of tubular epithelial cells and brush border losses of proximal tubules decreased in the RG treatment group (RHDS: 3(2–3)). (i) (x20)–(j) (x40): The IR+AM+RG combined treatment group showed a decrease in atypical glomeruli and necrotic tubules. In addition, it is observed that the structures of the brush-like edges of the proximal tubules are typical (RHDS: 1.5(1–2)).

Table 3. Immunohistochemical (IHC) positivity scoring result (median (25%–75% interquartile range).

Group	Tunel positivity score	Caspase-3 positivity score	8-OHdG positivity score
Control	0(0-0)	0(0-0)	0(0-0)
IR	2.5(2-3)[a]	3(2-3)[a]	3(2-3)[a]
IR + AM	1(1-1)[a,b]	1(1-1)[a,b]	1(0-1)[c,b]
IR + RG	1(1-2)[a,b]	1(1-2)[a,b]	1(1-2)[a,b]
IR+AM+RG	1(1-1)[a,b]	1(1-1)[a,b]	1(0.5–1)[a,b]

[a]p = .000; Compared to the control group.
[b]p = .000; Compared to the IR administration group.
[c]p = .01; Compared to the control group.
Kruskal Wallis/Tamhane T2 test.

enlargement of the renal tubules, glomerular atrophy, dilatation in Bowman's capsules, and leukocyte infiltration.[14] In their study of whole-body exposure to 5-Gy IR in a single fraction, Elkady et al. (2016) observed necrosis and tubular cast formation in tubular epithelial cells.[12] In trials in which the entire body was subject to 6-Gy radiation in a single fraction, Mercantepe et al. (2019) observed a rise in the surface areas of the proximal and distal tubules, as well as renal corpuscles with an atrophic glomerular structure.[10] Similarly in the current study, a single dose of whole-body 6-Gy x-irradiation caused diffuse necrotic tubules accompanying diffuse vacuolization in the epithelial cells of proximal and distal tubules.

Similar effects have been reported to occur in clinical phases following whole-body irradiation.[34] These necrotic tubules may appear alongside the development of progressive kidney disease, characterized by glomerular mesangial sclerosis and tubular degradation.[16] Common brush boundary losses have also been observed in the proximal tubules. In the current study, moderate rates of atypical glomerular structures were also observed. Considering the results of this and previous studies, it may be concluded that radiation exposure may cause nephrotoxicity and related complications that can persist for several years.[12,14,17] While leukocyte infiltration was observed in previous studies investigating the long-term effects of IR on the kidney, leukocyte infiltration was not observed in the present acute study.

Despite the histopathological changes observed in kidney tissue resulting from x-irradiation, the underlying damage mechanism has not been fully comprehended yet. However, recent research has indicated that x-irradiation increases levels of free oxygen radicals by inducing lipid peroxidation.[35] ROS has been observed to occur in cells subjected to IR, and the cell membrane exposed to these ROS is a natural target for free radical reactions due to its strong affinity for membrane lipids.[9,18] Various studies have stated that MDA levels increase in tissues exposed to radiation.[10,27] Likewise, in the current study, kidney tissue MDA levels showed an increase after 6 Gy irradiation. Various pieces of research have observed decreases in levels of GSH, a major defender of the organism against oxidative stress occurring in tissues exposed to IR and also an important marker of oxidative stress.[9,19] This may have resulted from the increased use of the antioxidant system to detoxify the free radicals produced after IR exposure.[12] Consistent with previous studies, the change in GSH in the present study decreased in the IR group. Studies have demonstrated that oxidative stress occurring in tissues after radiation triggers apoptotic mechanisms and increases the number of cells undergoing apoptosis.[10] Caspase-3 is a cysteine-protease group enzyme that plays an important role during apoptosis and is an important apoptotic marker.[36] Several studies have reported that the amount of caspase-3 in the organism increases significantly after irradiation.[37] Mercantepe et al. (2019) suggested that IR activated caspase-3 in renal tubule cells and enhanced the amount of apoptosis. In the present study, in which the whole body was exposed to 6 Gy IR, caspase-3 positivity was observed in the epithelial cells of the proximal and distal tubules in sections from the IR group. ROS, which increased after IR exposure, not only causes DNA damage in the cell but also raises levels of 8- OHdG, an important marker of oxidative stress. An increase in 8-OHdG has been described as an important biomarker in the case of cancer and degenerative alterations.[38] In the current study, 8-OHdG positivity was significantly lowered in the proximal and distal tubules of the AM, RG, and AM+RG groups compared to the IR group.

Numerous studies have revealed that substances with antioxidant and anti-inflammatory activities also possess radioprotective qualities, and various cytoprotective medicines have been produced accordingly.[39] AM is the most widely used synthetic radioprotectant, which reduces the exposure of healthy tissues without lowering the use of radiation in tumor tissues. When AM is given before radiotherapy or chemotherapy, it accumulates faster in normal tissues than in malignant tissues with low ALP expression. It can therefore protect healthy cells approximately 100 times better than cancer cells with low drug accumulation.[21]

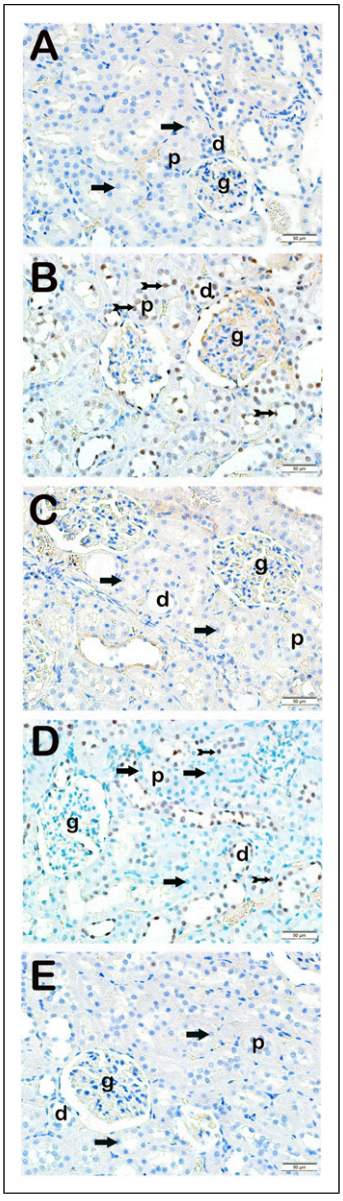

Figure 2. Representative light microscopic image of sections of kidney tissue incubated with the Tunnel kit. Glomerule (g), Proximal tubule (p), Distal tubule (d). (a) (x20): Tubular epithelial cells (arrow) are seen in kidney tissue slices from the control group (Tunnel positivity score: 0). (0-0). (b) (x20): Tunnel positivity (tailed arrow) is observed in the epithelial cells of the proximal and distal tubules in the sections of the IR application group (Tunnel positivity score: 2.5(2-3). (c) (x20): In the sections of the AM treatment group, decreased Tunnel positivity in the epithelial cells of the proximal and distal tubules is observed (arrow) (Tunnel positivity score: 1(1–1). (d) (x20): In the kidney tissue sections of the RG treatment group, it is observed that the epithelial cells of the proximal and distal tubules that show Tunnel positivity are decreased (arrow) (Tunnel positivity score: 1 (1–2). (e) (x20): In the kidney tissue sections of the IR+AM+RG combined treatment group, it is observed that the epithelial cells of the proximal and distal tubules that show Tunnel positivity are decreased (arrow) (Tunnel positivity score: 1(1–1).

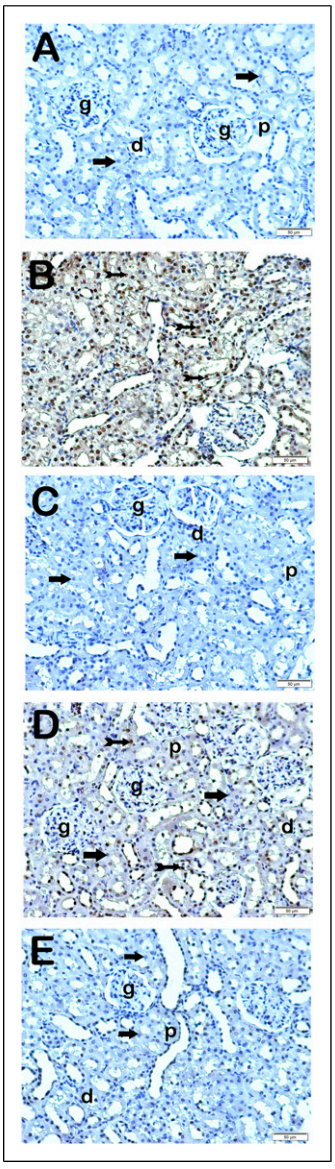

Figure 3. Representative light microscopic view of sections of kidney tissue incubated with caspase-3 primary antibody. Glomerule (g), Proximal tubule (p), Distal tubule (d). (a) (x20): It is observed that tubular epithelial cells (arrow) are typical in kidney tissue sections of the control group (Caspase-3 Positivity Score: 0(0–0.5). (b) (x20): Caspase-3 positivity is observed in the epithelial cells of the proximal and distal tubules in the sections of the IR application group (tailed arrow) (Caspase-3 Positivity Score: 0(0–0.5). (c) (x20): It is observed that Caspase-3 positivity is decreased in epithelial cells of proximal and distal tubules in sections of AM treatment group (arrow) (Caspase-3 Positivity Score: 0(0-0.5). (d) (x20): The number of Caspase-3-positive epithelial cells in proximal and distal tubules is reduced in kidney tissue sections from the RG therapy group (arrow) (Caspase-3 Positivity Score: 0(0–0.5). (e) (x20): In the kidney tissue sections of the IR+AM+RG combined treatment group, decreased epithelial cells of the proximal and distal tubules showing Caspase-3 positivity are observed (arrow) (Caspase-3 Positivity Score: 0(0–0.5).

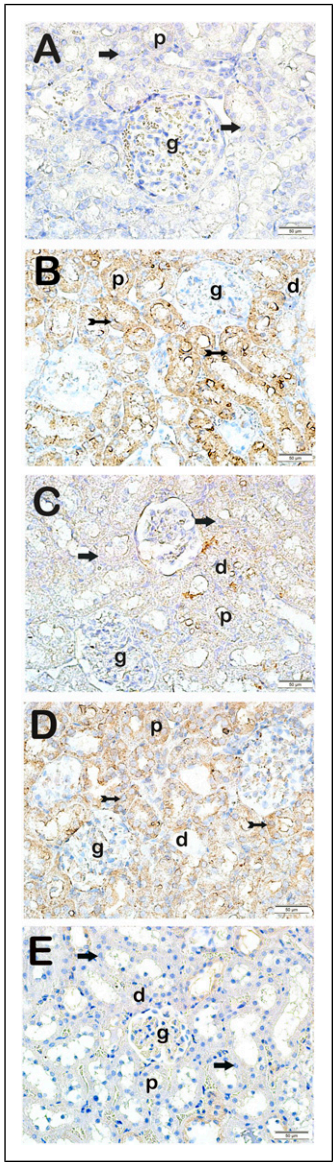

Figure 4. Representative light microscopic view of sections of kidney tissue incubated with 8-OHdG primary antibody. Glomerule (g), Proximal tubule (p), Distal tubule (d). (a) (x20): Tubular epithelial cells (arrow) are seen in kidney tissue slices from the control group (8-OHdG positive score: 0). (0–0). (b) (x20): In the sections of the IR application group, 8-OHdG positivity is observed in the epithelial cells of the proximal and distal tubules (tailed arrow) (8-OHdG positivity score: 3(2–3). (c) (x20): It is observed that 8-OHdG positivity is decreased in epithelial cells of proximal and distal tubules in sections of AM treatment group (arrow) (8-OHdG positivity score: 1(0–1). (d) (x20): In the kidney tissue sections of the RG treatment group, it is observed that the epithelial cells of the proximal and distal tubules, which show 8-OHdG positivity, are decreased (arrow) (8-OHdG positivity score: 1 (1–2). (e) (x20): The epithelial cells of the proximal and distal tubules, which display 8-OHdG positivity, are diminished (arrow) in the kidney tissue sections of the IR+AM+RG combination treatment group (8-OHdG positivity score: 1). (0.5–1).

AM removes IR-induced free radicals by increasing the environmental hydrogen concentration. In consequence, it exerts a radioprotective effect by lowering free radical DNA damage.

Previous studies have reported that AM increases GSH levels while reducing those of tissue MDA.[11,40] Undeger et al. revealed that rats exposed to 10 Gy IR exhibited higher levels of thiobarbituric acid-reactive substances, a biomarker of MDA.[41] Those authors also reported an increase in DNA chain breaks. In their scintigraphic evaluation of rat kidney tissues exposed to single-fraction 6-Gy IR, Uguzalp-Kaldır et al. confirmed that AM exhibits a radioprotective effect on the kidney. At the same time, they observed diminished radiation-induced histological alterations in kidney tissue.[26]

RG is used as a natural radioprotectant due to its strong antioxidant and anti-inflammatory properties.[42,43] Previous research has indicated that RG exerts a radioprotective effect either directly, by suppressing lipid peroxidation and scavenging free radicals, or indirectly by enhancing the activity of superoxide dismutase (SOD), a free radical scavenger enzyme.[12] According to Cho et al. (2019), RG activates antioxidant enzymes responsible for scavenging oxygen radicals, the by-products of cell metabolism.[23] Li et al. (2020) reported that RG eliminated ROS, reduced lipid peroxidation, and suppressed apoptosis.[44] Ginseng has also been shown to reduce the activity of phospholipase A2, responsible for lipid peroxidation. Similarly in the present study, the increase in MDA levels and decrease in GSH levels in IR group kidney tissues after IR exposure were significantly reversed compared to the IR group in the AM-only, RG-only, and AM+RG treatment groups. In the light of previous research, and the findings of the present study, AM, and RG can be employed to reduce the adverse effects of 6- Gy IR due to their radioprotective effects.

Mercantepe et al. (2018) suggested that AM suppressed caspase-3 expression and reduced apoptosis in renal tubular epithelial cells.[30] In addition, Özden et al. (2013) reported that AM reduces caspase-3 expression in tubular cells caused by a single dose of whole-body 8-Gy irradiation.[27] Cho et al. (2019) demonstrated that RG may be beneficial in repairing ionizing radiation-induced colon damage by inhibiting caspase-3 expression.[23] Chang et al. (2014) examined the protective effects of RG on radiation-induced oral mucositis through a single dose of 20 Gy IR to the whole body.[45] Those authors concluded that RG suppressed caspase-mediated apoptosis by inhibiting the caspase-3-dependent apoptotic signal transmission pathway. Similarly, in the present study, only AM, only RG, and AM+RG all decreased the numbers of apoptotic cells caused by IR in renal tubular epithelial cells compared to the IR group.

The biochemical, histopathological, and immunohistochemical findings from this experimental study confirmed the protective effects of AM and RG against the toxic effect

of IR on kidney tissues. In addition, previous research has shown that amifostine has side effects such as hypertension and hypocalcemia, the mechanism of which is as yet unknown.[46] On the other hand, there are no known side effects of red ginseng unless used in excess.[47]

According to Renal Histopathological Damage Scoring; The RG group was found to be significant compared to the IR group at a level close to the AM group. There was less damage in the AM+RG combined group than in the AM and RG groups alone. Mansour et al. (2013) stated in their study, we think that the low MDA value of the combined group and the increase in the total thiol level, depending on RG, may cause this situation. We think that the low MDA value of the combined group and the increase in the total thiol level may cause this situation.[25] In addition, although there was no significant difference between the treatment groups (AM, RG, AM+RG) in terms of IHC scores, it was found that the negative effect of IR decreased significantly in the treatment groups. Similar results were found by Cho et al. (2019) also reported that RG suppresses caspase-mediated apoptosis.[23] The absence of side effects during combined use also reveals the antioxidant effect of RG as a natural radioprotectant.

This study has some limitations to this study. In particular, x-irradiation was applied using a device employed in radiotherapy clinics, together with the most common protocol and dosage. Our research, therefore, needs to be supported by other studies including different dosages, mRNA transcript levels, and protein levels of genes involved in the apoptotic pathway and application durations. In addition, saline was applied via gavage application in the control groups to simulate potential complications resulting from drug administration and to eliminate the inaccurate evaluations that these may cause.

X-irradiation triggered acute kidney injury by causing an increase in free oxygen radicals and caspase-3 expression in renal tissue. On the other hand, AM, and RG both alone and in combination (AM+RG) exhibited a nephroprotective effect by suppressing apoptosis by reducing oxidative stress and caspase-3 expression by raising GSH levels and lowering MDA concentrations. Further studies involving other oxidative stress enzymes and compounds, as well as inflammation and apoptotic parameters are now needed.

Conclusion

6-Gy ionizing radiation enhanced MDA, 8-OHdG, and caspase-3 expression while decreasing renal tissue GSH levels. Significant histopathological changes in renal tubular cells were also observed. While GSH levels significantly increased in the treatment groups, a decrease was observed in the expression of KHDS, MDA, 8-OHdG, and caspase-3. For this reason, ROS-scavenging antioxidants may represent a promising treatment for avoiding renal damage in patients receiving IR.

Author contributions

HY and YK conceived and designed the research. HY and HS conducted the experiments. YK, HY, and TM contributed new reagents or analytical tools. AY, LT, TM, and HS analyzed the data, and HY, YK, and TM wrote the manuscript, SYR ırradiation procedure designed. All authors read and approved the final text.

Declaration of conflicting interests

The author(s) declared no potential conflicts of interest with respect to the research, authorship, and/or publication of this article.

Funding

The author(s) disclosed receipt of the following financial support for the research, authorship, and/or publication of this article: The Scientific Research Projects Unit of the University of Health Sciences and grant number 2020/136.

Ethical approval

All animals were cared for by the principles outlined in the National Institutes of Health Guidelines for the Care and Use of Laboratory Animals. The RTEU Local Animal Care Committee (Rize, Turkey) approved the study (protocol no. 2020/38-30.10.2020).

Data availability

The datasets used and/or analyzed during the current study are available from the corresponding author upon reasonable request.

ORCID iDs

Hamit Yilmaz https://orcid.org/0000-0002-8324-1891
Levent Tumkaya https://orcid.org/0000-0002-2814-5194

Supplemental Material

Supplemental material for this article is available online.

References

1. Sung H, Ferlay J, Siegel RL, et al. Global cancer statistics 2020: GLOBOCAN estimates of incidence and mortality worldwide for 36 cancers in 185 countries. *CA Cancer J Clin* 2021; 71: 209–249.
2. Wyld L, Audisio RA and Poston GJ. The evolution of cancer surgery and future perspectives. *Nat Rev Clin Oncol* 2015; 12: 115–124.
3. Lu Z, Zheng X, Ding C, et al. Deciphering the biological effects of radiotherapy in cancer cells. *Biomolecules* 2022; 12: 1167.
4. Liu W, Chen B, Zheng H, et al. Advances of nanomedicine in radiotherapy. *Pharmaceutics* 2021; 13: 1–31.
5. Gotwals P, Cameron S, Cipolletta D, et al. Prospects for combining targeted and conventional cancer therapy with immunotherapy. *Nat Rev Cancer* 2017; 17: 286–301.

6. Luke JJ, Flaherty KT, Ribas A, et al. Targeted agents, and immunotherapies: optimizing outcomes in melanoma. *Nat Rev Clin Oncol* 2017; 14: 463–482.
7. Thariat J, Hannoun-Levi J-M, Sun Myint A, et al. Past, present, and future of radiotherapy for the benefit of patients. *Nat Rev Clin Oncol* 2012; 10: 52–60.
8. Ceylan T, Kaymak E, Cantürk F, et al. Research on the protective effect of caffeic acid phenethyl ester on testicular damage caused by cisplatin. *Turkish J Med Sci* 2020; 50: 2032–2039.
9. Yahyapour R, Shabeeb D, Cheki M, et al. Radiation protection and mitigation by natural antioxidants and flavonoids: implications to radiotherapy and radiation disasters. *Curr Mol Pharmacol* 2018; 11: 285–304.
10. Mercantepe T, Topcu A, Rakici S, et al. The radioprotective effect of N-acetylcysteine against x-radiation-induced renal injury in rats. *Environ Sci Pollut Res* 2019; 26: 29085–29094.
11. Kucuktulu E. Protective effect of melatonin against radiation induced nephrotoxicity in rats. *Asian Pac J Cancer Prev* 2012; 13: 4101–4105.
12. Elkady A and Ibrahim I. Protective effects of erdosteine against nephrotoxicity caused by gamma radiation in male albino rats. *Hum Exp Toxicol* 2016; 35: 21–28.
13. Dawson LA, Kavanagh BD, Paulino AC, et al. Radiation-associated kidney injury. *Int J Radiat Oncol Biol Phys* 2010; 76: 108–115.
14. Talebpour Amiri F, Hamzeh M, Naeimi RA, et al. Radioprotective effect of atorvastatin against ionizing radiation-induced nephrotoxicity in mice. *Int J Radiat Biol* 2018; 94: 106–113.
15. Havasi A and Borkan SC. Apoptosis and acute kidney injury. *Kidney Int* 2011; 80: 29–40.
16. Aloy B, Janus N, Isnard-Bagnis C, et al. Toxicité rénale des anticancéreux. *Néphrologie & Thérapeutique* 2021; 17: 553–563.
17. Yahyapour R, Motevaseli E, Rezaeyan A, et al. Reduction–oxidation (redox) system in radiation-induced normal tissue injury: molecular mechanisms and implications in radiation therapeutics. *Clin Transl Oncol* 2018; 20: 1–14.
18. Ekici K, Temelli O, Parlakpinar H, et al. Beneficial effects of aminoguanidine on radiotherapy-induced kidney and testis injury. *Andrologia* 2016; 48: 683–692.
19. Abou-zeid SM, El-bialy BE, El-borai NB, et al. Radioprotective effect of date syrup on radiation- induced damage in rats. *Sci Rep* 2018; 8: 1–10.
20. Ueno M, Matsumoto S, Matsumoto A, et al. Effect of amifostine, a radiation-protecting drug, on oxygen concentration in tissue measured by EPR oximetry and imaging. *J Clin Biochem Nutr* 2017; 60: 151–155.
21. King M, Joseph S, Albert A, et al. Use of amifostine for cytoprotection during radiation therapy: a review. *Oncology* 2020; 98: 61–80.
22. Jung SW, Kim HJ, Lee BH, et al. Effects of Korean red ginseng extract on busulfan-induced dysfunction of the male reproductive system. *J Ginseng Res* 2015; 39: 243–249.
23. Cho HT, Kim JH, Heo W, et al. Explosively puffed ginseng ameliorates ionizing radiation-induced injury of colon by decreasing oxidative stress-related apoptotic cell execution in mice. *J Med Food* 2019; 22: 490–498.
24. El Adham EK, Hassan AI and Dawoud MM Evaluating the role of propolis and bee venom on the oxidative stress induced by gamma rays in rats. *Sci Rep* 2022; 12: 1–22.
25. Mansour HH. Protective effect of ginseng against gamma-irradiation-induced oxidative stress and endothelial dysfunction in rats. *EXCLI J* 2013; 12: 766–777.
26. Uguzalp-Kaldir M, Yürüt-Çaloglu V, Coşar-Alas R, et al. Prevention of radiation-induced liver and kiney toxicity: a role for amifostine. *Turkish J Oncol* 2007; 22: 1–6.
27. Özen A, Tastekin E, Parlar S, et al. PO-0909: comparison of protective effect of melatonin and amifostine on acute renal damage caused by ionizing radiation. *Radiother Oncol* 2013; 106: S352.
28. Suh S-O, Jin K and Cho M-Y. Prospective study for Korean red ginseng extract as an immune modulator following a curative surgery in patients with advanced colon cancer. *J Ginseng Res* 2007; 31: 54–59.
29. Rojas DB, Gemelli T, De Andrade RB, et al. Administration of histidine to female rats induces changes in oxidative status in cortex and hippocampus of the offspring. *Neurochem Res* 2012; 37: 1031–1036.
30. Mercantepe F, Mercantepe T, Topcu A, et al. Protective effects of amifostine, curcumin, and melatonin against cisplatin-induced acute kidney injury. *Naunyn Schmiedebergs Arch Pharmacol* 2018; 391: 915–931.
31. Ohkawa H, Ohishi N and Yagi K. Assay for lipid peroxides in animal tissues by thiobarbituric acid reaction. *Anal Biochem* 1979; 95: 351–358.
32. Ellman GL. Tissue sulfhydryl groups. *Arch Biochem Biophys* 1959; 82: 70–77.
33. Sung MJ, Kim DH, Jung YJ, et al. Genistein protects the kidney from cisplatin-induced injury. *Kidney Int* 2008; 74: 1538–1547.
34. Gil Marques F, Poli E, Malaquias J, et al. Erratum: low doses of ionizing radiation activate endothelial cells and induce angiogenesis in peritumoral tissues. *Radiother OncologyRadiother Oncol* 2019; 141151(256–261): 322–327. DOI: 10.1016/j.radonc.2019.06.035.
35. Yahyapour R, Amini P, Rezapoor S, et al. Targeting of inflammation for radiation protection and mitigation. *Curr Mol Pharmacol* 2018; 11: 208–210.
36. Mercantepe T, Kalkan Y, Tumkaya L, et al. Protective effects of tumor necrosis factor alpha inhibitors on methotrexate-induced pancreatic toxicity. *Adv Clin Exp Med* 2018; 27. DOI: 10.17219/acem/68967.
37. Kiang JG, Smith JT, Anderson MN, et al. Hemorrhage enhances cytokine, complement component 3, and caspase-3, and regulates microRNAs associated with intestinal damage after whole-body gamma-irradiation in combined injury. *PLoS One* 2017; 12: 1–25.

38. Liang H, Huang J, Huang Q, et al. Biochemical and biophysical research communications pharmacological inhibition of Rac1 exerts a protective role in ischemia/reperfusion-induced renal fibrosis. *Biochem Biophys Res Commun* 2018; 503: 2517–2523.
39. Hosseinimehr SJ, Ahmadi A, Beiki D, et al. Protective effects of hesperidin against genotoxicity induced by 99mTc-MIBI in human cultured lymphocyte cells. *Nucl Med Biol* 2009; 36: 863–867.
40. Uzal C, Durmus-Altun G, Caloglu M, et al. The protective effect of amifostine on radiation-induced acute pulmonary toxicity: detection by 99mTc-DTPA transalveolar clearances. *Int J Radiat Oncol Biol Phys* 2004; 60: 564–569.
41. Ündeğer Ü, Giray B, Zorlu AF, et al. Protective effects of melatonin on the ionizing radiation induced DNA damage in the rat brain. *Exp Toxicol Pathol* 2004; 55: 379–384.
42. Lee TK, Johnke RM, Allison RR, et al. Radioprotective potential of ginseng. *Mutagenesis* 2005; 20: 237–243.
43. Lee DY, Park CW, Lee SJ, et al. Anti-cancer effects of panax ginseng berry polysaccharides via activation of immune-related cells. *Front Pharmacol* 2019; 10: 1–11.
44. Li X, Chu S, Lin M, et al. Anticancer property of ginsenoside Rh2 from ginseng. *Eur J Med Chem* 2020; 203: 112627.
45. Chang JW, Choi JW, Lee BH, et al. Protective effects of Korean red ginseng on radiation-induced oral mucositis in a preclinical rat model. *Nutr Cancer* 2014; 66: 400–407.
46. Singh VK and Seed TM. The efficacy and safety of amifostine for the acute radiation syndrome. *Expert Opin Drug Saf* 2019; 18: 1077–1090.
47. Ran X, Dou D, Chen H, et al. The correlations of adverse effect and tonifying effect of ginseng medicines. *J Ethnopharmacol* 2022; 291: 115113.